UC Davis

UC Davis Previously Published Works

Title

Protective spin-labeled fluorenes maintain amyloid beta peptide in small oligomers and limit transitions in secondary structure

Permalink

https://escholarship.org/uc/item/5972h7pb

Journal

Biochimica et Biophysica Acta, 1854(12)

ISSN

0006-3002

Authors

Altman, Robin
Ly, Sonny
Hilt, Silvia
et al.

Publication Date

2015-12-01

DOI

10.1016/j.bbapap.2015.09.002

Peer reviewed

eScholarship.org Powered by the California Digital Library
University of California

Author Manuscript

Author Manuscript

Author Manuscript

Author Manuscript

HHS Public Access

Author manuscript

Biochim Biophys Acta. Author manuscript; available in PMC 2016 December 01.

Published in final edited form as:

Biochim Biophys Acta. 2015 December ; 1854(12): 1860–1870. doi:10.1016/j.bbapap.2015.09.002.

Protective spin-labeled fluorenes maintain amyloid beta peptide in small oligomers and limit transitions in secondary structure

Robin Altman[1,‡], **Sonny Ly**[2,‡], **Silvia Hilt**[1], **Jitka Petrlova**[1], **Izumi Maezawa**[3], **Tamás Kálai**[4], **Kálmán Hideg**[4], **Lee-Way Jin**[3], **Ted A. Laurence**[2], and **John C. Voss**[1,*]

[1]Department of Biochemistry & Molecular Medicine, University of California Davis, Davis, CA 95616

[2]Physical and Life Science Directorate, Lawrence Livermore National Laboratory, Livermore, CA 94550

[3]M.I.N.D. Institute and Department of Pathology and Laboratory Medicine, University of California Davis, Sacramento, CA 95817, USA

[4]Institute of Organic and Medicinal Chemistry, University of Pécs, H-7624 Pécs, Szigeti st. 12. Pécs, Hungary

Abstract

Alzheimer's disease is characterized by the presence of extracellular plaques comprised of amyloid beta (Aβ) peptides. Soluble oligomers of the Aβ peptide underlie a cascade of neuronal loss and dysfunction associated with Alzheimer's disease. Single particle analyses of Aβ oligomers in solution by fluorescence correlation spectroscopy (FCS) were used to provide real-time descriptions of how spin-labeled fluorenes (SLFs; bi-functional small molecules that block the toxicity of Aβ) prevent and disrupt oligomeric assemblies of Aβ in solution. Furthermore, the circular dichroism (CD) spectrum of untreated Aβ shows a continuous, progressive change over a 24-hour period, while the spectrum of Aβ treated with SLF remains relatively constant following initial incubation. These findings suggest the conformation of Aβ within the oligomer provides a complementary determinant of Aβ toxicity in addition to oligomer growth and size. Although SLF does not produce a dominant state of secondary structure in Aβ, it does induce a net reduction in beta secondary content compared to untreated samples of Aβ. The FCS results, combined with electron paramagnetic resonance spectroscopy and CD spectroscopy, demonstrate SLFs can inhibit the growth of Aβ oligomers and disrupt existing oligomers, while retaining Aβ as a population of smaller, yet largely disordered oligomers.

*jcvoss@ucdavis.edu.

‡R.A. and S.L. contributed equally to this work

Publisher's Disclaimer: This is a PDF file of an unedited manuscript that has been accepted for publication. As a service to our customers we are providing this early version of the manuscript. The manuscript will undergo copyediting, typesetting, and review of the resulting proof before it is published in its final citable form. Please note that during the production process errors may be discovered which could affect the content, and all legal disclaimers that apply to the journal pertain.

Author Manuscript Author Manuscript Author Manuscript Author Manuscript

Keywords

amyloid beta; oligomer; spin-labeled fluorene; secondary structure; fluorescence correlation spectroscopy; circular dichroism spectroscopy

1. Introduction

Alzheimer's disease (AD) is a progressive, neurodegenerative disease of aging resulting in gradual loss of cognitive function. Although the primary cause of AD is still unknown, the defining histopathological features of the disease are well-established. AD is characterized by the presence of two distinct features: insoluble extracellular amyloid beta (Aβ) plaques, and intracellular neurofibrillary tangles resulting from aggregates of hyperphosphorylated *tau*, a microtubule-associated protein. Aβ plaques are generated from the aggregation of soluble Aβ peptides that are formed when γ and β secretases cleave amyloid precursor protein (APP), a constitutively expressed transmembrane protein. These Aβ peptides possess an inherently disordered nature, which leaves them prone to progressive aggregation as oligomers, then proto-fibrils and fibrils, and finally mature plaques.

While a central role of Aβ in Alzheimer's disease is well-established, mechanistic studies over the past decade have focused on its soluble form, as the presence of amyloid plaques containing fibrillar, insoluble forms of Aβ were found to poorly align with the severity of Alzheimer's disease symptoms. Measurements taken *in vivo* and in cell culture have demonstrated the soluble, oligomeric state of Aβ (AβO) results in greater neuronal toxicity and impairment compared to the peptide in its fibrillar assembly [1-6]. The physiochemical properties of soluble Aβ are driven by its intrinsic disorder [7], which drives dynamic flux in both the oligomeric state and the structure of the assembled peptides. Since AβO acts as a moving target, the examination of this problem is furthered by methods that can capture dynamic states of biomolecules in solution [8, 9].

Soluble, non-fibrillar Aβ assemblies have been implicated as the primary cause of synaptic dysfunction and cognitive decline in AD. Identification of the particular conformational species responsible for these deleterious effects has been challenging due to the enormous heterogeneity of Aβ assemblies. However, a growing body of evidence suggests a relationship between toxicity, size, and surface hydrophobicity of amyloid aggregates, with maximum toxicity attributed to aggregates with a high surface-to-volume ratio [1, 10-14]. Antibodies have been selected to discriminate between conformational states of Aβ, with the A11 antibody reactive against neurotoxic oligomers of amyloidogenic species, and the OC immunoglobulin recognizing more compact and less toxic assemblies [5]. *In vivo* studies investigating the neurotoxicity of different Aβ species have identified a range of candidates based on oligomer size, including low molecular mass (< 10 kDa) Aβ oligomers [6, 15], as well as larger oligomers (> 50 kDa) [16] that cause detrimental effects on cognitive ability.

A major impediment to the development of anti-Aβ compounds for AD therapy is that essentially 100% of large-molecule drugs and greater than 98% of small-molecule drugs fail to cross the blood brain barrier (BBB) [17]. In addition, extracellular and intraneuronal AβO seem to exist in a dynamic equilibrium, with toxicity arising from both pools [18]. Thus,

Author Manuscript Author Manuscript Author Manuscript Author Manuscript

high cell permeability should also be considered necessary for an effective AβO antagonist. We have identified fluorene compounds, based on a highly rigid tricyclic fluorene ring originally developed as potential PET and SPECT imaging agents, on the basis of their amyloid affinity and blood brain barrier permeability [19], that are able to permeate cells, inhibit Aβ aggregation and neutralize the toxicity of soluble AβO [20]. More recently, we have synthesized bi-functional fluorenes by attaching nitroxides to the fluorene compound (Figure 1) [21]. We found the protective effect of these spin-labeled fluorenes (SLFs) is superior to the fluorene template and derives from the targeted antioxidant activity of the compound's nitroxide moiety [22]. Thus the increased potency of the SLF can be ascribed to its ability to address both conformational and oxidative stress [23] aspects of AβO toxicity.

In this work, we apply fluorescence correlation spectroscopy (FCS) to monitor the effect of the SLF compound on the size of Aβ assemblies in solution. FCS is a powerful technique for studying dynamic biochemical interactions *in vitro* and in cells [24-26]. In FCS, random diffusion of fluorescent molecules into and out of a femtoliter laser excitation volume leads to fluctuations in fluorescence intensity. Correlations calculated from recorded fluorescence signals reveal diffusion and binding properties of the molecules. For diffusion of a single species, the timescale at which the correlation function decays to half its amplitude gives the diffusion time, τ_D. Binding to other molecules or structures may be detected as changes in diffusion time, which are reflected by a shift in the autocorrelation curve. With precise knowledge of τ_D and laser beam waist, ω, the diffusion coefficient and hydrodynamic radius can be determined. Thus FCS provides a real-time, in-solution approach that is particularly useful in the study of protein aggregation processes inherent to neurodegenerative disorders [27-30]. Here, we apply FCS to better understand the manner in which SLFs to modulate Aβ toxicity as correlated to its aggregation, disaggregation and oligomeric stability, demonstrating the potential of this approach in identifying agents suitable for counteracting the molecular pathogenesis of AD.

2. Materials and Methods

2.1 Materials

Hexafluoro-2-propanol (HFIP) was purchased from Sigma-Aldrich (St. Louis, MO). Dimethyl sulfoxide (DMSO) was purchased from Fisher Scientific (Pittsburgh, PA). Atto 647N NHS ester was obtained from Fluka Analytical, Sigma-Aldrich (St. Louis, MO). $Aβ_{(1-40)}$ peptide was purchased from Bachem (catalog number H-1194, Torrance, CA). Amyloid-beta peptide (1-40) containing a TOAC spin label at position 26 ($Aβ^{(26TOAC)}$) was synthesized as described in [31]. Spin-labeled fluorene HO-4160 (SLF) and its diamagnetic derivative HO-4198 (SLF^{dm}) were synthesized as described in [21]. The structures of both are given in Figure 1.

2.2 Preparation of Amyloid β Peptide Samples

The Aβ peptide was dissolved in HFIP and incubated at room temperature with gentle rocking for 48-72 hours. SpeedVac or evaporation was then used to remove the HFIP, resulting in a monomeric Aβ pellet. Immediately before the given experiment, the HFIP-treated pellet was warmed to room temperature and dissolved in fresh DMSO to achieve a

Author Manuscript Author Manuscript Author Manuscript Author Manuscript

stock solution of 1 mM Aβ. To generate oligomers, the Aβ solution was then diluted into PBS (pH 7.4) buffer to a final concentration of 40 μM. The 40 μM solution was allowed to incubate at room temperature for the indicated times to produce oligomers. As demonstrated previously [20, 22, 31], these oligomeric preparations are A11-positive oligomers [4], with a 40 μM solution producing particles of ~10 nm at 4-hours by AFM imaging.

2.3 Cell Viability

Neuronal toxicity was accessed using the Neuro-2a (N2a) cell line [32]. Cells were plated at a density of 2.5×10^5 cells/well in a 12-well plate in medium containing 50 IU/mL penicillin and 50 μg/mL streptomycin. The medium was composed of a mixture of 50% Dulbecco's Modified Eagle Medium supplemented with 4.5 mg/mL D-glucose, non-essential amino acids, 1 mM sodium pyruvate, and 10% (v /v) heat-inactivated fetal bovine serum, and 50% Opti-Minimal Essential Medium (without phenol red) from Gibco/BRL (Carlsbad, CA).

To measure the toxicity of $A\beta_{(1\text{-}40)}$ to N2a cells, a 0.1 mg pellet of HFIP-treated $A\beta_{(1\text{-}40)}$ was reconstituted in 10 μL DMSO. Oligomeric Aβ was obtained by dilution in PBS pH 7.4 to a final concentration of 1 mM and incubation for 24 hours. Aβ was then added with and without SLF to the growth media at final concentrations of 50 μM for Aβ and 4 μM for SLF. Cytotoxicity was determined using counts of viable cells based on Trypan blue exclusion. To verify the nontoxic nature of the SLF, cell viability was also determined following incubation with SLF alone up to a concentration of 10 μM. Statistical significance between groups was determined by one-way ANOVA on ranks using SigmaStat software (Systat Software Inc., San Jose, CA), where $p < 0.05$ was considered significant.

2.4 Labeling of Amyloid β Peptide Samples with Fluorescent Dye

To direct preferential labeling of the N-terminal amine group of Aβ, a 0.1 mg aliquot of peptide was dissolved in 10 μL DMSO and reacted at pH 7.0 with 3 μL Atto 647N NHS ester label (10 mM stock in DMSO) and 500 μL phosphate-buffered saline (PBS; 120 mM NaCl, 25 mM phosphate, pH 7.0). At this pH, the only appreciable level of unprotonated amine (capable of reacting with the NHS-ester probe) exists at the N-terminal α-amine, whereas >99% of the Lys ε-amines remain protonated at this pH [33]. The mixture incubated for 2 hours at room temperature, and the oligomeric species pelleted by centrifugation at 100,000 × *g*. To remove unreacted Atto probe, the pellet was washed 6 times with fresh PBS. After the final PBS wash was removed, HFIP was added to the labeled peptide and allowed to evaporate. The resulting pellet was stored at -20°C until use.

2.5 FCS Instrumentation

We conducted our experiments using a time-resolved confocal fluorescence microscope equipped with a 640 nm pulsed diode laser (PicoQuant, Germany) operating at a repetition rate of 20 MHz. Immediately prior to each measurement, fluorescently-labeled Aβ samples were diluted to a probe (Atto 647N NHS ester) concentration of 10 nM in PBS (pH 7.4). The laser was focused to a diffraction-limited spot of ~350 nm diameter by an Olympus 1.45 NA 100x oil objective to a height of 5 μm above a glass coverslip surface. The average power was 20 μW at the sample. The fluorescence emission was split by a dichroic mirror

Author Manuscript Author Manuscript Author Manuscript Author Manuscript

(600DCXR, Chroma Tech. Corp., Bellows Falls, VT), spectrally filtered with emission bandpass filters (HQ680/75 m, Chroma Tech. Corp., Bellows Falls, VT), and detected by two avalanche photodiode detectors (SPCM-AQR-14, PerkinElmer, Waltham, MA). The signals were processed by a time-correlated single-photon counting board (PicoHarp300, PicoQuant, Germany), operating in time-tagged time-resolved (TTTR) mode. The TTTR mode of the data acquisition records the photon arrival time from the last excitation pulse (micro-time) with 50-ps relative time resolution, and the photon arrival time from the start of the experiment (macro-time) with 100-ns absolute time resolution. Correlations were calculated using the SymPhoTime software package (PicoQuant GmbH, Berlin). Data were fitted to maximize χ^2 using the Levenberg-Marquardt least-squares method.

2.6 Surface-Bound Species Removal Algorithm

A common problem in taking accurate FCS measurements is the presence of large intensity spikes. These spikes can be due to formation of large aggregates, or the tendency of molecules to stick to glass surfaces, as commonly occurs in measurements involving Aβ. These large fluorescent bursts, if not corrected for, can skew the results of the analysis, resulting in an autocorrelation curve that is mostly dominated by that particular diffusion event. Removal of these intensity spikes is necessary for accurate FCS measurements. To eliminate these surface-bound species from our data, we implemented a custom algorithm that cuts a portion of the intensity time trace that contains photon bursts greater than 10x the average signal. The remaining portion of the time trace is then stitched back into the original time trace for correlation analysis. A detailed description of excluding signal from adhered species is given in [34].

2.7 Circular Dichroism Spectroscopy

Circular dichroism spectroscopy (CD) measurements were performed on a Jasco J-715 spectropolarimeter equipped with a Peltier temperature control (Quantum Northwest) set to 25°C. Since DMSO absorbs strongly in the far UV and overlaps with protein absorption spectra, acetonitrile, a UV transparent solvent, was used to reconstitute the Aβ. Dried pellets of HFIP-treated Aβ (0.2 mg) were dissolved in 7 μL acetonitrile, and 3.5 μL of the peptide was added to 300 μL of PBS (pH 7.4) plus 3 μL of acetonitrile (with or without SLF) and allowed to incubate for the indicated times. CD spectra of both samples were measured at 0 hours under identical parameters. Care was taken to utilize the same minimal amount of acetonitrile in control and +SLF conditions, as the fraction of disordered structure in Aβ is affected by solvent [35-37]. In order to minimize the strong far-UV absorption by Cl^-, NaF was used in place of NaCl for PBS solutions in all CD measurements. For samples analyzed after amorphous aggregate removal, 0.32 mg/mL of Aβ peptide was combined with either SLF or acetonitrile vehicle for 15 minutes and then centrifuged at 15,000 × g for 5 minutes. Aβ concentrations in the supernatants were determined using a NanoDrop reader with the extinction coefficient estimated from the peptide sequence. After centrifugation, the Aβ concentrations were 0.04 mg/ML and 0.14 mg/mL for the control and +SLF samples, respectively. CD spectra of the supernatants were then measured at the same time intervals and using the same parameters.

Author Manuscript Author Manuscript Author Manuscript Author Manuscript

For spectral acquisition, samples were placed in a 1 mm quartz cuvette and CD spectra were collected by signal averaging three scans in the region 190 to 260 nm using a scan speed of 20 nm/min, bandwith of 1 nm and response time of 4 sec. Prior to analysis, all spectra were baseline-subtracted from the appropriate background buffer containing either the SLF alone or the solvent vehicle (the background signals were generally indistinguishable. The percent of secondary structure was estimated by deconvolution using the BeStSel CD analysis program[38], which can be accessed on line at http://bestsel.elte.hu.

2.8 Electron Paramagnetic Resonance Spectroscopy

EPR measurements were carried out on preparations of Aβ containing a TOAC spin-labeled amino acid substituted at position 26 of the $A\beta_{(1\text{-}40)}$ peptide ($A\beta^{(26TOAC)}$). Spin-coupling among proximal TOAC labels was attenuated by dissolving HFIP-treated peptide in DMSO and combining 1 part $A\beta^{(26TOAC)}$ with 3 parts wild-type $A\beta_{(1\text{-}40)}$ to generate a spin-diluted DMSO stock of peptide. Oligomeric samples for EPR were then prepared by dilution of the DMSO stock solution into cold PBS buffer (pH 7.4) for a total Aβ peptide concentration of 80 μM (containing 20 μM paramagnetic $A\beta^{(26TOAC)}$). All EPR measurements were performed using a JEOL FA-100 X-band spectrometer fitted with a loop-gap resonator. Approximately 4 μL of each sample was loaded into a sealed borosilicate glass capillary tube (Fiber Optic Center, Inc., New Bedford, MA). The spectra were obtained by averaging three 2-minute scans with a sweep width of 100 G at a microwave power of 3 mW recorded at room temperature. The modulation amplitude was optimized according to the natural line width of the TOAC spin probe. Spectra were processed using Origin 7 software (OriginLab Corporation, Northampton, MA).

3. Results

3.1 SLF blocks the toxicity of Aβ added to N2a cells

We previously used a neuronal cell culture model capable of inducible over-expression of APP to show SLF protects against the toxicity of intraneuronal Aβ [22]. To confirm that SLF converts Aβ to a less toxic species, we added SLF to oligomeric Aβ (AβO) and added the mixture exogenously to cultured N2a neurons. As shown in Figure 2, no viable cells remained three days after AβO addition. However, by adding SLF to the AβO sample prior to its application to the N2a cells, the health and viability of the cells after three days resembles that of the control cells.

3.2 SLF inhibits Aβ oligomer growth in solution as monitored by FCS

A primary feature of the Aβ peptide is its propensity to aggregate over time in aqueous solution. Most studies on this process have focused on the stages apparent in amyloid fibril formation, which involves the adoption of highly ordered cross-beta structure that typically occurs over a 2-4 week incubation *in vitro*. In order to monitor the Aβ assembly state associated with higher cellular toxicity, we used FCS to measure the diffusion time of Aβ in solution over the first 4 hours of incubation in the presence and absence of SLF. We used a sample solution consisting of 40 μM Aβ labeled with Atto 647 dye. For each FCS measurement, a small volume of this sample was diluted to less than 1 nM in phosphate-buffered saline (PBS) to ensure that the excitation volume contains an average of one

Author Manuscript Author Manuscript Author Manuscript Author Manuscript

molecule or less, which gives a high signal-to-noise ratio for these conditions while still allowing single molecule burst analysis on surface-bound species. We take the FCS measurement immediately after dilution, within one minute or less, to minimize the dead-time. Although simple binary association of SLF can dissociate during this period, aggregates do not, as their dissociation would show up as a shift towards a rapid diffusion time on the autocorrelation curve. This is not observed in our analysis. The data were recorded for two minutes at each time interval.

At the start of the experiment (time zero), monomeric Aβ is the predominant species, with a fast diffusion time of 40 μs (Figure 3, black curve; Figure 4). Significant aggregation occurs within the first 4 hours as indicated by the large shift to a slow diffusion time of 7.1 ms (Figure 3, light gray curve; Figure 4). After 4 hours, a much slower phase of aggregation is observed, with a 24-hour incubation producing a diffusion time of 9.3 ms (Figure 4). In contrast, when a solution of 40 μM Aβ was mixed with 40 μM SLF compound, the diffusion time was much faster (Figure 3, red curve).

Fits of the correlation decays provide diffusion rates (τ_D), with optimization indicative of single- or multi-component samples. Samples treated with SLF fit best with a two-component model consisting of a fast species with a correlation time of ≤ 0.1 ms and a slower species on the order of 4-7 ms (Figure 4; Table S1). The exception is AβO aggregated over 24 hours, which lacks a significant contribution from the faster component until it has been in the presence of SLF for 4 hours (Figure 4; Table S1). For all samples displaying two components, the slower component predominates, representing 60-85% of the species (Table S1). At 4 hours, the sample with SLF fits best with a two-component diffusion species model, where 15% of the total fraction is from τ_1 = 85 μs and 85% is from τ_2 = 4.5 ms. The emergence of two diffusion times is likely due to the interaction with SLF that breaks the complex into particles with a wider distribution of sizes. τ1 represents smaller (on the order of a monomer or dimer) Aβ particles while the majority of the peptide remains oligomeric. The χ^2 of these fits were between 1.1 and 1.5.

3.3 SLF disrupts larger oligomers of Aβ

We also monitored the effect of SLF on a solution containing oligomerized Aβ to test the ability of the molecule to disrupt pre-formed Aβ aggregates. First we looked at the effect of adding SLF to a 4-hour AβO incubation (Figure 5, red curve). The diffusion time for this sample is 4.2 ms, a substantial decrease from τ = 7.1 ms prior to SLF addition (Figure 4). This indicates the SLF converts AβO into smaller (more rapidly diffusing) species. The rate of diffusion for the 4-hour AβO sample treated with SLF is on the order of samples containing SLF from the onset of peptide incubation in buffer (i.e., 4-5 ms). However, when the same experiment is carried out on 24-hour AβO, the diffusion correlation time only decreases to 6.6 ms (Figure 4; Figure 5, blue curve).

3.4 Photon burst analysis supports FCS analysis showing disruption of oligomerization

We performed burst analysis to analyze the intensity and width of each fluorescence burst corresponding to individual large oligomers. Larger oligomers lead to photon bursts with higher intensities and longer widths. A time trace for a 2-minute diffusion event is shown for

Author Manuscript Author Manuscript Author Manuscript Author Manuscript

Aβ alone and Aβ + SLF incubated together for 4 hours (Figure 6A). In the absence of SLF, Aβ displayed wider and more intense bursts due to the formation of large oligomers (black trace). In the presence of SLF, the intensity of these fluorescent bursts decreased (red trace). Burst histograms were generated to show the number of events with a specific photon count (Figure 6B). The burst histogram is derived from the intensity time trace at 4 hours and counts all the photons within the burst regardless of the length of the burst. For free Aβ, there were many bursts containing over 500 counts, with some bursts approaching over 1000 counts due to rapid aggregation of Aβ. The mean time of each burst was 2.4 ms (Figure 6C) with some bursts extending beyond 50 ms. In contrast, the Aβ-SLF complex contained mostly smaller particles, thus the majority of bursts were less than 200 counts/ms with average burst width of 2.0 ms. In our analysis of all samples, extremely large bursts over 1000 counts/ms (Figure 6D) that are not a true representation of the species are removed with the surface-bound species removal algorithm. To summarize, Aβ alone resulted in large intensity bursts with large burst times, while the Aβ-SLF complex resulted in smaller burst intensity and shorter burst time. These observations, coupled with FCS measurements, demonstrate the ability of the SLF molecule to inhibit Aβ oligomerization.

3.5 SLF decreases the fraction of beta strand structure in oligomeric Aβ

In order to determine whether the complex oligomerization of Aβ observed by FCS reveals corresponding secondary structure changes, we measured the circular dichroism (CD) spectra of Aβ over a 24-hour time period. The spectral changes in oligomeric Aβ over 24 hours are complex (Figure 7A). The secondary structural values resulting from deconvolution are given in Table S2 and plotted in Figures 7C and 7D. The analysis of secondary structure contribution for untreated peptide reveals an increase in peptide disorder over the first 4 hours, and then a drop in the fraction of unstructured peptide at 24 hours (Figure 4C).

The effect of SLF on the time-dependent changes in Aβ secondary structure is shown in Figure 7B, with the deconvolution of secondary structure components plotted in Figure 7D. A notable difference compared to the spectra of the control sample is that the +SLF spectra display similarity for the 2- to 24-hour time points, with only modest changes occurring in the far-UV range. Regarding secondary structure content, the most obvious difference over all time points relative to control lies in the amplitudes of the unstructured components (lower in SLF) and the alpha components (higher in SLF). As shown in Figure 7D, SLF results in a substantial decrease in unstructured peptide over the first 4 hours, corresponding with a population converted into helical structure. However with time, the +SLF sample displays a rise in unstructured amplitude, which is mirrored by a decrease in alpha-helical content over 24 hours. In contrast, the beta and turn components are relatively unchanged over this same period. As discussed below, the lack of increase in beta structure for the +SLF sample at 24 hours is of significance, since the size of the oligomeric species determined by FCS is best correlated with its amount of beta structure determined by CD. This is also consistent with the nature of the 4-hour Aβ sample in the absence of SLF, which displays both the fastest correlation time and the lowest fraction of beta content.

Author Manuscript Author Manuscript Author Manuscript Author Manuscript

Previous CD analysis has demonstrated that the large amorphous aggregates formed by Aβ in aqueous solution generate a skewed CD spectrum, due to the ability of such species to absorb UV light, but not behave as CD-active chromophores [39, 40]. We therefore repeated CD analysis on Aβ sample cleared of such aggregates by centrifugation (see Methods). This procedure is particularly informative in that it provides another demonstration that SLF inhibits the formation of such aggregates, as ~3.5x more Aβ remains in the supernatant if SLF is present. As shown in Figure 8, removal of the amorphous aggregates affects both the control and +SLF CD spectra, although the effect is far more profound in the control sample, consistent with the SLF compound reducing the amount of large aggregates. With respect to the fractions of calculated secondary structure, the results are largely similar in that the primary difference between control and SLF-treated Aβ remains a lowered amount of beta structure in the latter.

3.6 SLF addition to 24-hour mature AβO produces a unique CD spectrum, with a decrease in the spectral intensity at the beta-I region compared to 24-hour Aβ lacking SLF treatment

As the FCS findings in Figure 3 show the ability of SLF to disrupt oligomers after 4 hours of treatment, as well as prevent their growth, we then looked at the secondary structure of the disrupted 24-hour oligomer. Fresh Aβ was incubated in PBS for 24 hours, treated with 40 μM SLF, incubated for another 4 hours, and then analyzed by CD spectroscopy. As shown in Figure 9, the CD spectrum of this sample is distinct from sample containing SLF from the onset of incubation. The secondary structure values resulting from deconvolution are shown in Table S2. Compared to the 24-hour sample with SLF present from the onset, the major effect of SLF addition to 24-hour Aβ is a decrease in the amount of unstructured Aβ. This is consistent with a mechanism where more structured forms of Aβ dissociate from oligomers in the presence of SLF.

3.7 Disassembly of 24-hour mature AβO is also evident by EPR

Electron paramagnetic resonance (EPR) spectroscopy of spin labels attached to Aβ has been used to resolve the arrangement of the peptide in fibrils [41] and oligomers [42, 43]. We have previously used the dynamics of a TOAC-incorporated spin label ($Aβ^{(26TOAC)}$) to show the SLF compound inhibits the time-dependent ordering of the Aβ peptide in aqueous solution [22]. In these measurements, spin-labeled Aβ is mixed with unlabeled Aβ (25% mole fraction of $Aβ^{(26TOAC)}$) to attenuate the spectral broadening arising from dipolar magnetic interaction among nearby spins in the oligomer. The EPR spectrum of $Aβ^{(26TOAC)}$ freshly added to PBS is shown in Figure 10A (black trace). To ascertain the ability of SLF to disrupt AβO of increasing maturity, we added the diamagnetic version of SLF (SLF^{dm}) so that only the $Aβ^{(26TOAC)}$ signal is observed by EPR. At the initial time point, addition of SLF^{dm} results in a slight broadening of the EPR spectrum, most likely due to the restriction of local dynamics induced by SLF^{dm} binding Figure 10A (red trace). After 24 hours in PBS, the spectum of $Aβ^{(26TOAC)}$ reveals considerable broadening, due largely to the slower correlation time of the larger aggregate (Figure 10B, black trace). However, addition of a stoichiometric amount of SLF^{dm} to the 24-hour sample alleviates much of this broadening (Figure 10B, red trace), consistent with a faster correlation time for $Aβ^{(26TOAC)}$ after SLF^{dm} treatment. These results support FCS results showing SLF^{dm} disrupts 24-hour oligomers of Aβ.

Author Manuscript Author Manuscript Author Manuscript Author Manuscript

3.8 Tightly packed AβO generated by Zn(II) are largely resistant to SLF disruption

To further probe the efficacy of SLF to disrupt AβO, we used Zn(II) to generate large, non-fibrillar aggregates of Aβ [44-46]. In addition to increasing the rate and size of Aβ aggregation, micromolar Zn(II) produces a highly stable form of aggregate that demonstrates resistance to protease treatment [47]. Because Zn(II) levels can be substantial (up to 60 μM) at the neuronal synapse, its profound physical effect on Aβ has been postulated to increase [46] and decrease [44, 48] the toxicity of Aβ (reviewed in [49]). As shown in Figure 11A, addition of stoichiometric (80 μM) Zn(II) to Aβ immediately results in a severely broadened EPR spectrum. Although the sample contains only 25% $A\beta^{(26TOAC)}$, dipolar interaction undoubtly contributes to the spectrum given the extent of broadening. This suggets a very close packing of Zn(II)-coordinated peptides. This effect becomes slightly more pronounced over 24 hours (Figure 11A). We then tested whether SLF^{dm} can disrupt Zn(II)-treated Aβ that has incubated for 4 hours. In contrast to the Zn(II)-free AβO sample (Figure 11B), addition of SLF^{dm} provides only marginal relief of the spectral broadening (Figure 10B, green trace). Finally, we also investigated whether including SLF^{dm} prior to Zn(II) addition is capable of blocking the metal-induced aggregation. As shown in Figure 11B (blue trace), Aβ pretreated with SLF^{dm} displays less spectral broadening than the Zn(II)-Aβ sample lacking SLF (Figure 11B, red trace), however the relief in broadening is on the order of what is observed when SLF^{dm} is added after a 4-hour incubation with Zn(II). Thus, while SLF^{dm} is capable of disrupting or blocking the growth of Aβ oligomers, at stoichiometric levels it shows marginal activity in the presence of Zn(II).

4. Discussion

The etiology of multiple neurodegenerative diseases stems from proteins or protein fragments containing poorly defined structural regions that aggregate and coalesce into insoluble deposits [50]. Efforts to elucidate the molecular pathology of such disorders are complicated not only by the heterogeneity of the toxic species, but also by the ability of these species to disrupt a range of cellular processes. For example, AβO appears to have multiple cellular targets [51], inducing not only neuronal apoptosis, but also neuronal functions such as outgrowth and synaptic signaling. Additionally, Aβ has been shown to impair glial cell function, including that of both astrocytes [52] and microglia [53]. Thus toxicity must be used in a broad sense for Aβ and other agents that propagate through intrinsic disorder and aggregation. The connection between structure and assembly is central to this problem, as aggregation affects secondary structure and secondary structure affects aggregation rates [7, 50]. Thus while several studies have correlated toxicity with a specific oligomeric state (e.g., [6, 16]), it is equally important to ascertain the structure (or lack thereof) and dynamics of Aβ in these assemblies.

The conversion of more recent *in situ* studies supports a more complex toxicity mechanism involving an “oligomeric soup” of Aβ species undergoing a dynamic equilibrium dominated by species heterogeneous in both size and secondary structure [54]. Early investigations of Aβ aggregation kinetics and structure exhibited variable conclusions regarding aggregate size/structure and the kinetics of aggregation [55-58]. As such, even slight differences in conditions and temporal variation can complicate comparative analyses. The lack of

Author Manuscript Author Manuscript Author Manuscript Author Manuscript

structural specificity is consistent with Aβ disrupting and dis-regulating multiple cellular processes, and the multi-factorial nature of AD in general. This complicates the design of biophysical studies as well, which can been simplified by manipulating solvent conditions and removing large amorphous aggregates by centrifugation prior to analysis [39, 40, 59, 60]. Although our experiments are challenged by the heterogenous nature of oligomeric Aβ, it is important to access the influence of structural modulators in the context of this dynamic equilibrium. While SLF limits both the progression of aggregation and the extent of secondary structural change over time, it does not convert Aβ into a well-defined oligomeric or structural state. Thus analyses using other biophysical tools capable of observing Aβ under equilibrium conditions, such as DLS [61, 62], are warranted.

CD spectra of Aβ are highly dependent on the experimental conditions, including the peptide concentration and version (1-40 or 1-42), solution temperature, ionic strength, and pH. Our measurements of early Aβ species in PBS buffer contain spectral features resembling β_{II}-class proteins, structures that are high in short, distorted beta strands and combined with a high degree of unordered backbone [63]. This contrasts with the CD spectra from β_I proteins, where adjacent strands are closely paired in H-bonding and generate a broad negative band centered around ~215 nm and a positive band at 197 nm [63]. Dominant pleated beta structure in $A\beta_{(1\text{-}40)}$ is typically achieved *in vitro* after 24 or more hours, during its slow maturation into protofibrils and adoption of a β_I-type CD spectrum, which becomes more characteristic after several days [64]. Additionally, after clearance of large amorphous aggregates Aβ treated with SLF displays CD features resembling the poly(Pro)II-type helix (i.e., a relatively sharp negative band at ~197 and a positive band in the >210 nm region). This CD pattern is not uncommon in unstructured peptides [65], and can be increased in Aβ at lower temperatures [66]. Since this signal was identified with residues in the N-terminal portion of Aβ [66], future studies can explore whether SLF has a larger conformational effect on this region of the peptide.

Our previous measurements showed SLF reduces ThT staining, the appearance of 10 nm particles in AFM, and spin magnetic coupling among spin labels incorporated into Aβ [22]. Thus we considered the possibility that SLF may act by blocking oligomer formation. However, while SLF clearly inhibits oligomer growth and decreases oligomer size, our FCS findings of oligomeric Aβ in the presence of SLF demonstrate a form of AβO with little-to-no toxicity. These results are in line with a study of tetracycline's effect on Aβ toxicity and oligomerization, where tetracycline was found to produce a stable distribution of soluble oligomers with low toxicity to cultured neurons [67]. FCS measurements also allow us to distinguish the SLF response of early oligomers (4 hours or less) from more mature oligomers (24 hours). Within the first 4 hours of oligomer formation, regardless of whether the SLF is added before or after peptide assembly, a similar (~ 4 ms) diffusion time is observed. Whereas following a 24-hour aggregation period, SLF does reduce diffusion times, but only to 6.6 ms. This is consistent with the distinct CD spectra of 24-hour Aβ in the presence of SLF, differentiated by whether the sample contains SLF from the onset of its incubation or the SLF is added at 24 hours.

Based on the FCS measurements, our treatment of cultured neurons with Aβ-SLF involved two oligomeric species of Aβ: ~70% having a molecular diameter on the order of 4-5 nm,

Author Manuscript Author Manuscript Author Manuscript Author Manuscript

and the remainder residing as a monomer or dimer. The fact that no effect on cell viability is observed with this mixture indicates a loss of toxicity for the SLF-Aβ mixture in either oligomeric state. The attenuation of AβO toxicity by SLF provides insight into the conformational elements within AβO that can be associated with cellular toxicity. Previous studies have identified the level of beta structure in AβO with increased toxicity [1, 36, 42, 66, 68, 69], including observations that the “arctic” mutations in Aβ increase beta structure within the oligomer [69, 70]. Notably, Cohen et al have proposed that the seeding of beta structure in soluble Aβ by fibril ends may represent a key molecular mechanism in AD pathology [68]. Our CD measurements are in agreement with this notion, in that SLF decreases beta structure in Aβ by ~10%, and can reduce the beta content within 24-hour mature AβO.

The ability to inhibit peptide aggregation and fibrilization has been found with other small molecules that show protective activities against Aβ toxicity [36, 71-73]. In the case of tetracycline, soluble Aβ is not dispersed into monomers, but maintains a supramolecular complex that remains soluble and stable over time [71]. This observation is particularly interesting, as the same study showed the peptide in complex with tetracycline retains very little beta sheet content, remaining in a disordered state. This observation, in addition to our finding that the most consistent effect of SLF on Aβ structure is its ability to hinder an increase in beta secondary structure, suggests oligomer size alone may not serve as a useful predictor of Aβ toxicity. Rather, the growth capability and/or the secondary structure within the oligomer are likely to be more informative metrics with respect to peptide toxicity.

As studies indicate the neurodegenerative effects of AD derive largely from the toxicity of soluble Aβ oligomers [1-6, 68], rational therapeutic interventions must focus on ameliorating the detrimental effects of these species. Our results demonstrate a novel class of bi-functional nitroxide-containing fluorene compounds, spin-labeled fluorenes or SLFs, have the ability to interfere with the oligomerization process and disrupt mature oligomers to produce less toxic species. We used fluorescence correlation spectroscopy to monitor the dynamic biochemical interactions between Aβ oligomers and SLFs in solution. Fluorescence correlation, electron paramagnetic resonance, and circular dichroism spectroscopic methods uniformly indicate SLFs slow the formation of Aβ oligomers and maintain Aβ as smaller species, disassemble mature oligomers, and lower the fraction of beta secondary structure in the largely dissordered oligomers. SLFs provide ideal candidates for AD therapeutics given their affinity for Aβ peptides and permeability to cells and the blood-brain barrier [19-22]. By further elucidating the interactions between SLFs and Aβ assemblies, our work provides insight into the potential of these compounds as anti-Aβ agents to help slow or prevent the progression of AD.

Supplementary Material

Refer to Web version on PubMed Central for supplementary material.

Author Manuscript Author Manuscript Author Manuscript Author Manuscript

Acknowledgments

We thank Prof. Gary Lorigan for the synthesis of TOAC-labeled Aβ. This work was in part supported by grant P30 AG010129 from the National Institutes of Health (JV) and grant OTKA 104956 from the Hungarian Research Fund (KH and TK).

References

1. Cheon M, Chang I, Mohanty S, Luheshi LM, Dobson CM, Vendruscolo M, Favrin G. Structural reorganisation and potential toxicity of oligomeric species formed during the assembly of amyloid fibrils. PLoS Comput Biol. 2007; 3:1727–1738. [PubMed: 17941703]
2. Dahlgren KN, Manelli AM, Stine WB Jr, Baker LK, Krafft GA, LaDu MJ. Oligomeric and fibrillar species of amyloid-beta peptides differentially affect neuronal viability. The Journal of biological chemistry. 2002; 277:32046–32053. [PubMed: 12058030]
3. Klein WL, Stine WB Jr, Teplow DB. Small assemblies of unmodified amyloid beta-protein are the proximate neurotoxin in Alzheimer's disease. Neurobiology of aging. 2004; 25:569–580. [PubMed: 15172732]
4. Kayed R, Head E, Thompson JL, McIntire TM, Milton SC, Cotman CW, Glabe CG. Common structure of soluble amyloid oligomers implies common mechanism of pathogenesis. Science. 2003; 300:486–489. [PubMed: 12702875]
5. Krishnan R, Goodman JL, Mukhopadhyay S, Pacheco CD, Lemke EA, Deniz AA, Lindquist S. Conserved features of intermediates in amyloid assembly determine their benign or toxic states. Proceedings of the National Academy of Sciences of the United States of America. 2012; 109:11172–11177. [PubMed: 22745165]
6. Shankar GM, Li S, Mehta TH, Garcia-Munoz A, Shepardson NE, Smith I, Brett FM, Farrell MA, Rowan MJ, Lemere CA, Regan CM, Walsh DM, Sabatini BL, Selkoe DJ. Amyloid-beta protein dimers isolated directly from Alzheimer's brains impair synaptic plasticity and memory. Nature medicine. 2008; 14:837–842.
7. De Simone A, Kitchen C, Kwan AH, Sunde M, Dobson CM, Frenkel D. Intrinsic disorder modulates protein self-assembly and aggregation. Proceedings of the National Academy of Sciences of the United States of America. 2012; 109:6951–6956. [PubMed: 22509003]
8. Teplow DB. On the subject of rigor in the study of amyloid beta-protein assembly. Alzheimers Res Ther. 2013; 5:39. [PubMed: 23981712]
9. Luheshi LM, Dobson CM. Bridging the gap: from protein misfolding to protein misfolding diseases. FEBS Lett. 2009; 583:2581–2586. [PubMed: 19545568]
10. Campioni S, Mannini B, Zampagni M, Pensalfini A, Parrini C, Evangelisti E, Relini A, Stefani M, Dobson CM, Cecchi C, Chiti F. A causative link between the structure of aberrant protein oligomers and their toxicity. Nat Chem Biol. 2010; 6:140–147. [PubMed: 20081829]
11. Baglioni S, Casamenti F, Bucciantini M, Luheshi LM, Taddei N, Chiti F, Dobson CM, Stefani M. Prefibrillar amyloid aggregates could be generic toxins in higher organisms. J Neurosci. 2006; 26:8160–8167. [PubMed: 16885229]
12. Bolognesi B, Kumita JR, Barros TP, Esbjorner EK, Luheshi LM, Crowther DC, Wilson MR, Dobson CM, Favrin G, Yerbury JJ. ANS binding reveals common features of cytotoxic amyloid species. ACS Chem Biol. 2010; 5:735–740. [PubMed: 20550130]
13. Silveira JR, Raymond GJ, Hughson AG, Race RE, Sim VL, Hayes SF, Caughey B. The most infectious prion protein particles. Nature. 2005; 437:257–261. [PubMed: 16148934]
14. Bucciantini M, Giannoni E, Chiti F, Baroni F, Formigli L, Zurdo J, Taddei N, Ramponi G, Dobson CM, Stefani M. Inherent toxicity of aggregates implies a common mechanism for protein misfolding diseases. Nature. 2002; 416:507–511. [PubMed: 11932737]
15. Cleary JP, Walsh DM, Hofmeister JJ, Shankar GM, Kuskowski MA, Selkoe DJ, Ashe KH. Natural oligomers of the amyloid-beta protein specifically disrupt cognitive function. Nat Neurosci. 2005; 8:79–84. [PubMed: 15608634]

Author Manuscript Author Manuscript Author Manuscript Author Manuscript

16. Lesne S, Koh MT, Kotilinek L, Kayed R, Glabe CG, Yang A, Gallagher M, Ashe KH. A specific amyloid-beta protein assembly in the brain impairs memory. Nature. 2006; 440:352–357. [PubMed: 16541076]
17. Pardridge WM. Blood-brain barrier delivery. Drug discovery today. 2007; 12:54–61. [PubMed: 17198973]
18. Oddo S, Caccamo A, Smith IF, Green KN, LaFerla FM. A dynamic relationship between intracellular and extracellular pools of Abeta. Am J Pathol. 2006; 168:184–194. [PubMed: 16400022]
19. Lee CW, Kung MP, Hou C, Kung HF. Dimethylamino-fluorenes: ligands for detecting beta-amyloid plaques in the brain. Nucl Med Biol. 2003; 30:573–580. [PubMed: 12900283]
20. Hong HS, Maezawa I, Budamagunta M, Rana S, Shi A, Vassar R, Liu R, Lam KS, Cheng RH, Hua DH, Voss JC, Jin LW. Candidate anti-Abeta fluorene compounds selected from analogs of amyloid imaging agents. Neurobiology of aging. 2010; 31:1690–1699. [PubMed: 19022536]
21. Kalai T, Petrlova J, Balog M, Aung HH, Voss JC, Hideg K. Synthesis and study of 2-amino-7-bromofluorenes modified with nitroxides and their precursors as dual anti-amyloid and antioxidant active compounds. Eur J Med Chem. 2011; 46:1348–1355. [PubMed: 21333407]
22. Petrlova J, Kalai T, Maezawa I, Altman R, Harishchandra G, Hong HS, Bricarello DA, Parikh AN, Lorigan GA, Jin LW, Hideg K, Voss JC. The influence of spin-labeled fluorene compounds on the assembly and toxicity of the abeta Peptide. PLoS One. 2012; 7:e35443. [PubMed: 22558151]
23. Sultana R, Butterfield DA. Role of oxidative stress in the progression of Alzheimer's disease. J Alzheimers Dis. 2010; 19:341–353. [PubMed: 20061649]
24. Ehrenberg M, Rigler R. Fluorescence correlation spectroscopy applied to rotational diffusion of macromolecules. Q Rev Biophys. 1976; 9:69–81. [PubMed: 1273258]
25. Koppel DE. Statistical accuracy in fluorescence correlation spectroscopy. Physical Rev A. 1974; 10:1938.
26. Magde D, Elson EL, Webb WW. Thermodynamic fluctuations in a reacting system: Measurement by fluorescence correlation spectroscopy. Phys Rev Lett. 1972; 29:705–708.
27. Joshi N, Basak S, Kundu S, De G, Mukhopadhyay A, Chattopadhyay K. Attenuation of the early events of alpha-synuclein aggregation: a fluorescence correlation spectroscopy and laser scanning microscopy study in the presence of surface-coated Fe3O4 nanoparticles. Langmuir. 2015; 31:1469–1478. [PubMed: 25561279]
28. Hochdorffer K, Marz-Berberich J, Nagel-Steger L, Epple M, Meyer-Zaika W, Horn AH, Sticht H, Sinha S, Bitan G, Schrader T. Rational design of beta-sheet ligands against Abeta42-induced toxicity. Journal of the American Chemical Society. 2011; 133:4348–4358. [PubMed: 21381732]
29. Mittag JJ, Milani S, Walsh DM, Radler JO, McManus JJ. Simultaneous measurement of a range of particle sizes during Abeta1-42 fibrillogenesis quantified using fluorescence correlation spectroscopy. Biochem Biophys Res Commun. 2014; 448:195–199. [PubMed: 24769478]
30. Nag S, Sarkar B, Bandyopadhyay A, Sahoo B, Sreenivasan VK, Kombrabail M, Muralidharan C, Maiti S. Nature of the amyloid-beta monomer and the monomer-oligomer equilibrium. The Journal of biological chemistry. 2011; 286:13827–13833. [PubMed: 21349839]
31. Petrlova J, Hong HS, Bricarello DA, Harishchandra G, Lorigan GA, Jin LW, Voss JC. A differential association of Apolipoprotein E isoforms with the amyloid-beta oligomer in solution. Proteins. 2011; 79:402–416. [PubMed: 21069870]
32. Hong HS, Maezawa I, Yao N, Xu B, Diaz-Avalos R, Rana S, Hua DH, Cheng RH, Lam KS, Jin LW. Combining the rapid MTT formazan exocytosis assay and the MC65 protection assay led to the discovery of carbazole analogs as small molecule inhibitors of Abeta oligomer-induced cytotoxicity. Brain research. 2007; 1130:223–234. [PubMed: 17157826]
33. Grimsley GR, Scholtz JM, Pace CN. A summary of the measured pK values of the ionizable groups in folded proteins. Protein Sci. 2009; 18:247–251. [PubMed: 19177368]
34. Persson G, Thyberg P, Sanden T, Widengren J. Modulation filtering enables removal of spikes in fluorescence correlation spectroscopy measurements without affecting the temporal information. J Phys Chem B. 2009; 113:8752–8757. [PubMed: 19492787]

Author Manuscript Author Manuscript Author Manuscript Author Manuscript

35. Barrow CJ, Yasuda A, Kenny PT, Zagorski MG. Solution conformations and aggregational properties of synthetic amyloid beta-peptides of Alzheimer's disease. Analysis of circular dichroism spectra. J Mol Biol. 1992; 225:1075–1093. [PubMed: 1613791]
36. Bartolini M, Bertucci C, Bolognesi ML, Cavalli A, Melchiorre C, Andrisano V. Insight into the kinetic of amyloid beta (1-42) peptide self-aggregation: elucidation of inhibitors' mechanism of action. Chembiochem. 2007; 8:2152–2161. [PubMed: 17939148]
37. Crescenzi O, Tomaselli S, Guerrini R, Salvadori S, D'Ursi AM, Temussi PA, Picone D. Solution structure of the Alzheimer amyloid beta-peptide (1-42) in an apolar microenvironment. Similarity with a virus fusion domain. Eur J Biochem. 2002; 269:5642–5648. [PubMed: 12423364]
38. Micsonai A, Wien F, Kernya L, Lee YH, Goto Y, Refregiers M, Kardos J. Accurate secondary structure prediction and fold recognition for circular dichroism spectroscopy. Proceedings of the National Academy of Sciences of the United States of America. 2015; 112:E3095–3103. [PubMed: 26038575]
39. Huang TH, Yang DS, Fraser PE, Chakrabartty A. Alternate aggregation pathways of the Alzheimer beta-amyloid peptide. An in vitro model of preamyloid. The Journal of biological chemistry. 2000; 275:36436–36440. [PubMed: 10961999]
40. Chiti F, Webster P, Taddei N, Clark A, Stefani M, Ramponi G, Dobson CM. Designing conditions for in vitro formation of amyloid protofilaments and fibrils. Proceedings of the National Academy of Sciences of the United States of America. 1999; 96:3590–3594. [PubMed: 10097081]
41. Torok M, Milton S, Kayed R, Wu P, McIntire T, Glabe CG, Langen R. Structural and dynamic features of Alzheimer's Abeta peptide in amyloid fibrils studied by site-directed spin labeling. The Journal of biological chemistry. 2002; 277:40810–40815. [PubMed: 12181315]
42. Wu JW, Breydo L, Isas JM, Lee J, Kuznetsov YG, Langen R, Glabe C. Fibrillar oligomers nucleate the oligomerization of monomeric amyloid beta but do not seed fibril formation. The Journal of biological chemistry. 2010; 285:6071–6079. [PubMed: 20018889]
43. Gu L, Liu C, Guo Z. Structural insights into Abeta42 oligomers using site-directed spin labeling. The Journal of biological chemistry. 2013; 288:18673–18683. [PubMed: 23687299]
44. Garai K, Sahoo B, Kaushalya SK, Desai R, Maiti S. Zinc lowers amyloid-beta toxicity by selectively precipitating aggregation intermediates. Biochemistry. 2007; 46:10655–10663. [PubMed: 17718543]
45. Bush AI, Pettingell WH, Multhaup G, Paradis M, Vonsattel JP, Gusella JF, Beyreuther K, Masters CL, Tanzi RE. Rapid induction of Alzheimer A beta amyloid formation by zinc. Science. 1994; 265:1464–1467. [PubMed: 8073293]
46. Noy D, Solomonov I, Sinkevich O, Arad T, Kjaer K, Sagi I. Zinc-amyloid beta interactions on a millisecond time-scale stabilize non-fibrillar Alzheimer-related species. Journal of the American Chemical Society. 2008; 130:1376–1383. [PubMed: 18179213]
47. Crouch PJ, Tew DJ, Du T, Nguyen DN, Caragounis A, Filiz G, Blake RE, Trounce IA, Soon CP, Laughton K, Perez KA, Li QX, Cherny RA, Masters CL, Barnham KJ, White AR. Restored degradation of the Alzheimer's amyloid-beta peptide by targeting amyloid formation. Journal of neurochemistry. 2009; 108:1198–1207. [PubMed: 19141082]
48. Kawahara M, Mizuno D, Koyama H, Konoha K, Ohkawara S, Sadakane Y. Disruption of zinc homeostasis and the pathogenesis of senile dementia. Metallomics. 2014; 6:209–219. [PubMed: 24247360]
49. Tougu V, Tiiman A, Palumaa P. Interactions of Zn(II) and Cu(II) ions with Alzheimer's amyloid-beta peptide. Metal ion binding, contribution to fibrillization and toxicity. Metallomics. 2011; 3:250–261. [PubMed: 21359283]
50. Dobson CM. The structural basis of protein folding and its links with human disease. Philos Trans R Soc Lond B Biol Sci. 2001; 356:133–145. [PubMed: 11260793]
51. Manzoni C, Colombo L, Bigini P, Diana V, Cagnotto A, Messa M, Lupi M, Bonetto V, Pignataro M, Airoldi C, Sironi E, Williams A, Salmona M. The molecular assembly of amyloid abeta controls its neurotoxicity and binding to cellular proteins. PLoS One. 2011; 6:e24909. [PubMed: 21966382]
52. Thal DR. The role of astrocytes in amyloid beta-protein toxicity and clearance. Exp Neurol. 2012; 236:1–5. [PubMed: 22575598]

Author Manuscript Author Manuscript Author Manuscript Author Manuscript

53. Krabbe G, Halle A, Matyash V, Rinnenthal JL, Eom GD, Bernhardt U, Miller KR, Prokop S, Kettenmann H, Heppner FL. Functional impairment of microglia coincides with Beta-amyloid deposition in mice with Alzheimer-like pathology. PLoS One. 2013; 8:e60921. [PubMed: 23577177]
54. Hubin E, van Nuland NA, Broersen K, Pauwels K. Transient dynamics of Abeta contribute to toxicity in Alzheimer's disease. Cell Mol Life Sci. 2014; 71:3507–3521. [PubMed: 24803005]
55. Hilbich C, Kisters-Woike B, Reed J, Masters CL, Beyreuther K. Aggregation and secondary structure of synthetic amyloid beta A4 peptides of Alzheimer's disease. J Mol Biol. 1991; 218:149–163. [PubMed: 2002499]
56. Burdick D, Soreghan B, Kwon M, Kosmoski J, Knauer M, Henschen A, Yates J, Cotman C, Glabe C. Assembly and aggregation properties of synthetic Alzheimer's A4/beta amyloid peptide analogs. The Journal of biological chemistry. 1992; 267:546–554. [PubMed: 1730616]
57. Tomski SJ, Murphy RM. Kinetics of aggregation of synthetic beta-amyloid peptide. Arch Biochem Biophys. 1992; 294:630–638. [PubMed: 1567217]
58. Snyder SW, Ladror US, Wade WS, Wang GT, Barrett LW, Matayoshi ED, Huffaker HJ, Krafft GA, Holzman TF. Amyloid-beta aggregation: selective inhibition of aggregation in mixtures of amyloid with different chain lengths. Biophys J. 1994; 67:1216–1228. [PubMed: 7811936]
59. Kumar A, Paslay LC, Lyons D, Morgan SE, Correia JJ, Rangachari V. Specific soluble oligomers of amyloid-beta peptide undergo replication and form non-fibrillar aggregates in interfacial environments. The Journal of biological chemistry. 2012; 287:21253–21264. [PubMed: 22544746]
60. Lindgren M, Sorgjerd K, Hammarstrom P. Detection and characterization of aggregates, prefibrillar amyloidogenic oligomers, and protofibrils using fluorescence spectroscopy. Biophys J. 2005; 88:4200–4212. [PubMed: 15764666]
61. Cizas P, Budvytyte R, Morkuniene R, Moldovan R, Broccio M, Losche M, Niaura G, Valincius G, Borutaite V. Size-dependent neurotoxicity of beta-amyloid oligomers. Arch Biochem Biophys. 2010; 496:84–92. [PubMed: 20153288]
62. Pryor NE, Moss MA, Hestekin CN. Unraveling the early events of amyloid-beta protein (Abeta) aggregation: techniques for the determination of Abeta aggregate size. Int J Mol Sci. 2012; 13:3038–3072. [PubMed: 22489141]
63. Sreerama N, Woody RW. Structural composition of betaI- and betaII-proteins. Protein Sci. 2003; 12:384–388. [PubMed: 12538903]
64. Walsh DM, Hartley DM, Kusumoto Y, Fezoui Y, Condron MM, Lomakin A, Benedek GB, Selkoe DJ, Teplow DB. Amyloid beta-protein fibrillogenesis. Structure and biological activity of protofibrillar intermediates. The Journal of biological chemistry. 1999; 274:25945–25952. [PubMed: 10464339]
65. Adzhubei AA, Sternberg MJ, Makarov AA. Polyproline-II helix in proteins: structure and function. J Mol Biol. 2013; 425:2100–2132. [PubMed: 23507311]
66. Danielsson J, Jarvet J, Damberg P, Graslund A. The Alzheimer beta-peptide shows temperature-dependent transitions between left-handed 3-helix, beta-strand and random coil secondary structures. FEBS J. 2005; 272:3938–3949. [PubMed: 16045764]
67. Airoldi C, Colombo L, Manzoni C, Sironi E, Natalello A, Doglia SM, Forloni G, Tagliavini F, Del Favero E, Cantu L, Nicotra F, Salmona M. Tetracycline prevents Abeta oligomer toxicity through an atypical supramolecular interaction. Org Biomol Chem. 2011; 9:463–472. [PubMed: 21063627]
68. Cohen SI, Linse S, Luheshi LM, Hellstrand E, White DA, Rajah L, Otzen DE, Vendruscolo M, Dobson CM, Knowles TP. Proliferation of amyloid-beta42 aggregates occurs through a secondary nucleation mechanism. Proceedings of the National Academy of Sciences of the United States of America. 2013; 110:9758–9763. [PubMed: 23703910]
69. Lam AR, Teplow DB, Stanley HE, Urbanc B. Effects of the Arctic (E22-->G) mutation on amyloid beta-protein folding: discrete molecular dynamics study. Journal of the American Chemical Society. 2008; 130:17413–17422. [PubMed: 19053400]
70. Paivio A, Jarvet J, Graslund A, Lannfelt L, Westlind-Danielsson A. Unique physicochemical profile of beta-amyloid peptide variant Abeta1-40E22G protofibrils: conceivable neuropathogen in arctic mutant carriers. J Mol Biol. 2004; 339:145–159. [PubMed: 15123427]

Author Manuscript Author Manuscript Author Manuscript Author Manuscript

71. Airoldi C, Colombo L, Manzoni C, Sironi E, Natalello A, Doglia SM, Forloni G, Tagliavini F, Del Favero E, Cantu L, Nicotra F, Salmona M. Tetracycline prevents Abeta oligomer toxicity through an atypical supramolecular interaction. Org Biomol Chem. 2010; 9:463–472. [PubMed: 21063627]

72. Yang F, Lim GP, Begum AN, Ubeda OJ, Simmons MR, Ambegaokar SS, Chen PP, Kayed R, Glabe CG, Frautschy SA, Cole GM. Curcumin inhibits formation of amyloid beta oligomers and fibrils, binds plaques, and reduces amyloid in vivo. The Journal of biological chemistry. 2005; 280:5892–5901. [PubMed: 15590663]

73. Hong HS, Rana S, Barrigan L, Shi A, Zhang Y, Zhou F, Jin LW, Hua DH. Inhibition of Alzheimer's amyloid toxicity with a tricyclic pyrone molecule in vitro and in vivo. Journal of neurochemistry. 2009; 108:1097–1108. [PubMed: 19141069]

Glossary

AD	Alzheimer's disease
Aβ	amyloid beta
AβO	amyloid beta oligomer
SLF	spin-labeled fluorene
FCS	fluorescence correlation spectroscopy
CD	circular dichroism spectroscopy
EPR	electron paramagnetic resonance spectroscopy
APP	amyloid precursor protein

Author Manuscript Author Manuscript Author Manuscript Author Manuscript

Highlights

- The small molecule SLF blocks Aβ toxicity, inhibits oligomer growth and disrupts larger oligomers.
- SLF arrests Aβ in a distribution of smaller oligomers and decreases the amount of beta strand content, although the species remain largely disordered.
- After 24-hours in the presence of SLF Aβ oligomers are about half the size of control sample and contain ~10% less beta structure compared to untreated Aβ.
- The ability of FCS to sample single molecules and assemblies in solution provides a sensitive and quantitative method to evaluate modulators of Aβ oligomerization.

Author Manuscript Author Manuscript Author Manuscript Author Manuscript

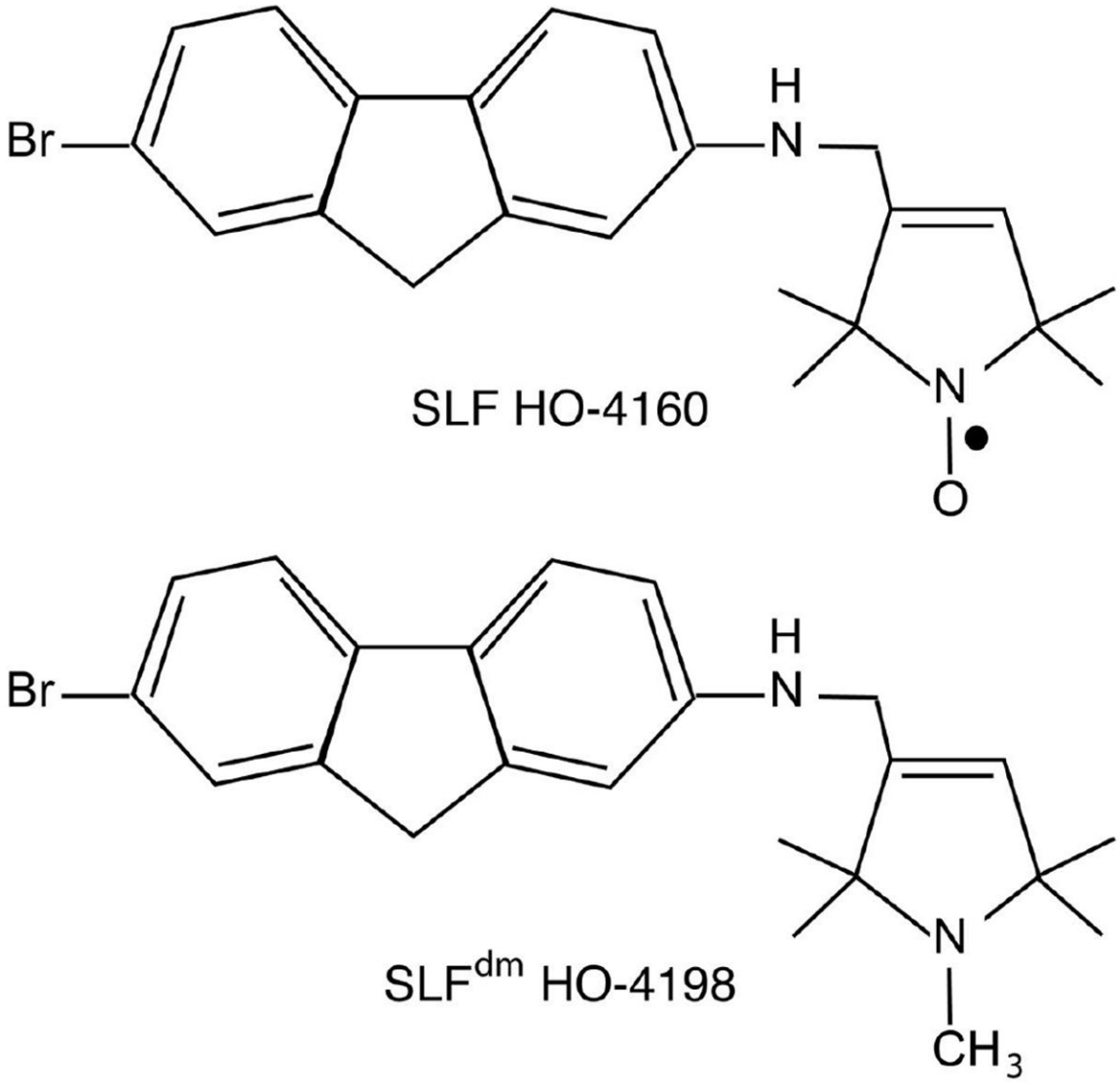

Figure 1.
Structures of the paramagnetic (top) and diamagnetic (bottom) SLF compounds used in this study.

Author Manuscript Author Manuscript Author Manuscript Author Manuscript

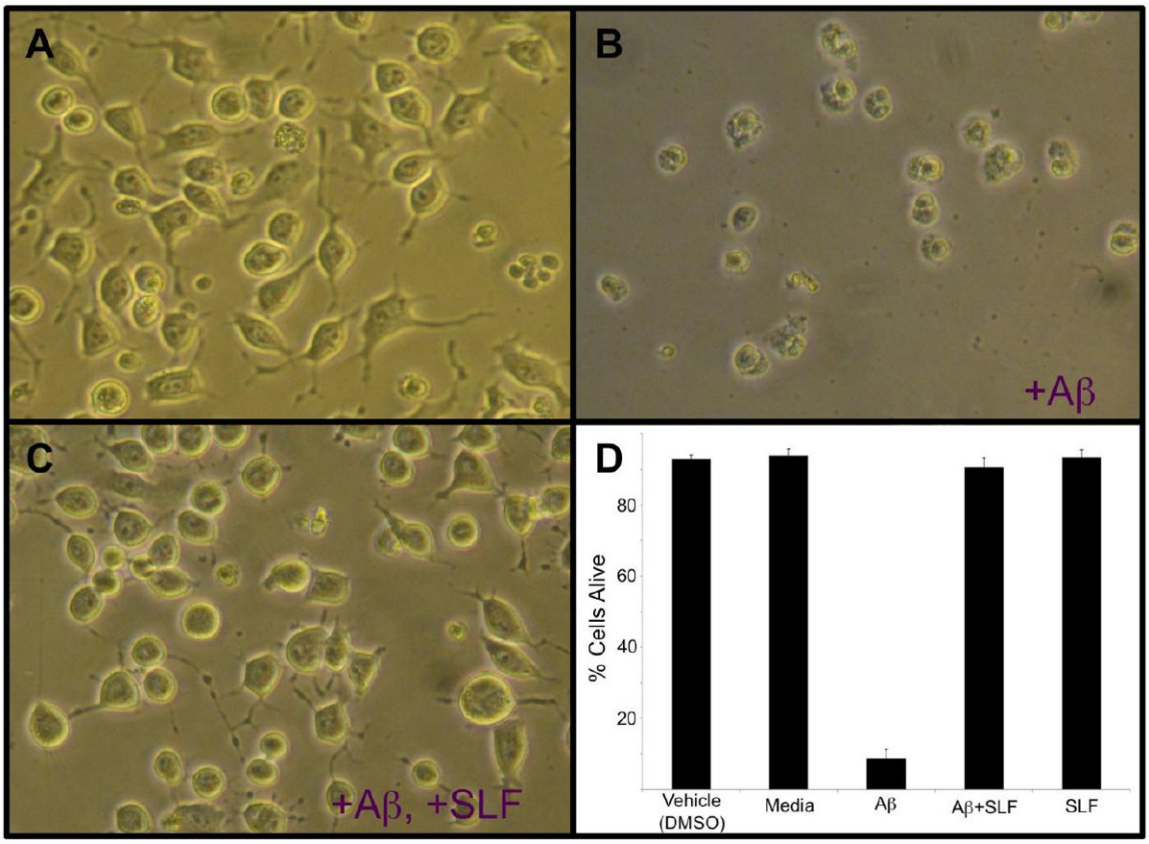

Figure 2. SLF protects N2a cells against exogenous Aβ

Shown are images of N2a cells after three days with treatment of either DMSO vehicle control (**A**) or addition of exogenous AβO (Aβ incubated for 24 hours in PBS to generate oligomers prior to addition to the culture media at a final concentration of 50 μM; **B**). Aβ toxicity is readily apparent from both the decreased cell count and the poor morphology of cells in panel **B**. When Aβ is combined with 4 μM SLF prior to culture application (panel **C**), cell viability resembles the control in panel **A**. N2a cell viability was quantified using Trypan blue exclusion (panel **D**). SLF alone was tested at 10 μM. Results are expressed as means ± SD of percent cells alive following treatment. * $p < 0.05$ compared to media treatment.

Author Manuscript Author Manuscript Author Manuscript Author Manuscript

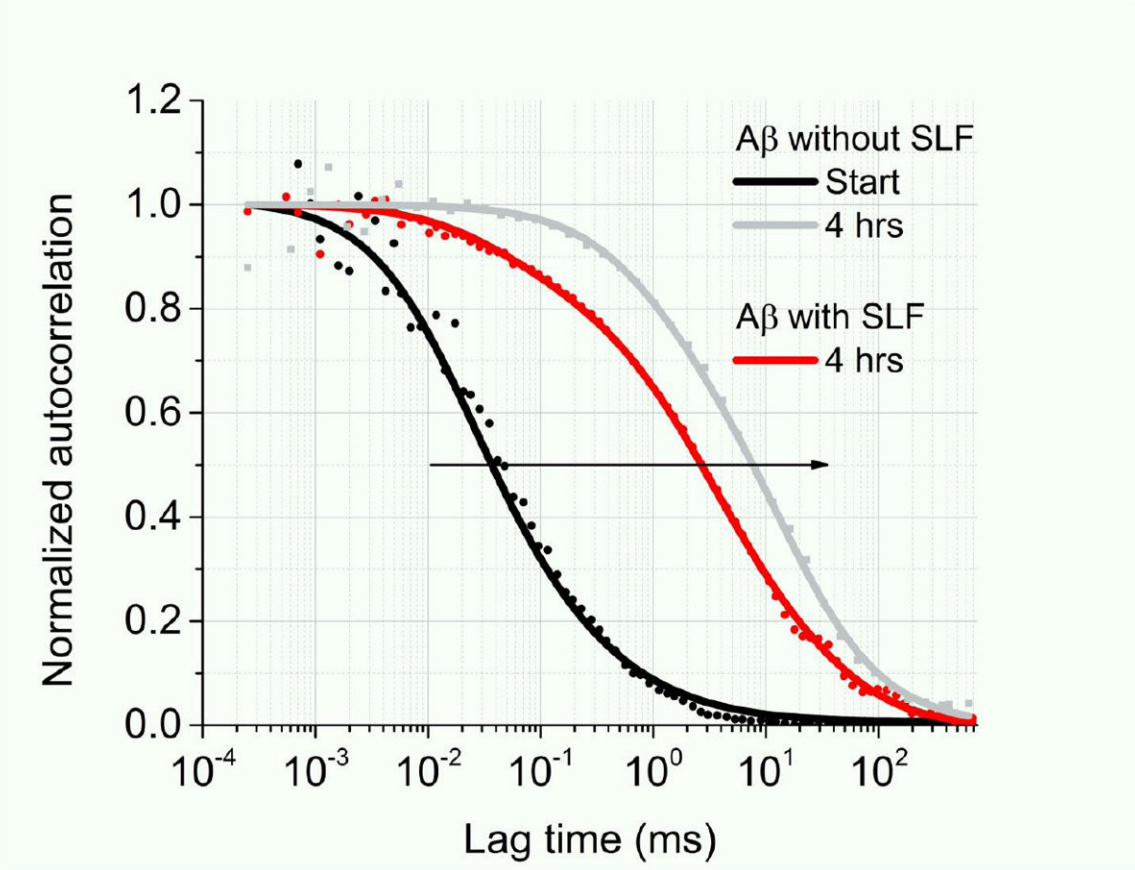

Figure 3. FCS measurements of 40 μM Aβ in the absence and presence of 40 μM SLF

The diffusion time at the start of the measurement is 40 μs due to the presence of monomeric or dimeric forms of Aβ (black curve). For free Aβ, self-aggregation causes the FCS curve to shift to a very slow diffusion time (gray solid arrow) of over 7 ms at the 4-hour mark. In the presence of SLF, the FCS curve shows a much faster diffusion time. With the addition of SLF, the FCS curve fits best with a two-component diffusion species model, where 15% of the total fraction is from τ_1 = 85 μs and 85% is from τ_2 = 4.5 ms. τ_1 is from small Aβ particles while τ_2 is mostly dominated by Aβ+SLF complexes.

Author Manuscript Author Manuscript Author Manuscript Author Manuscript

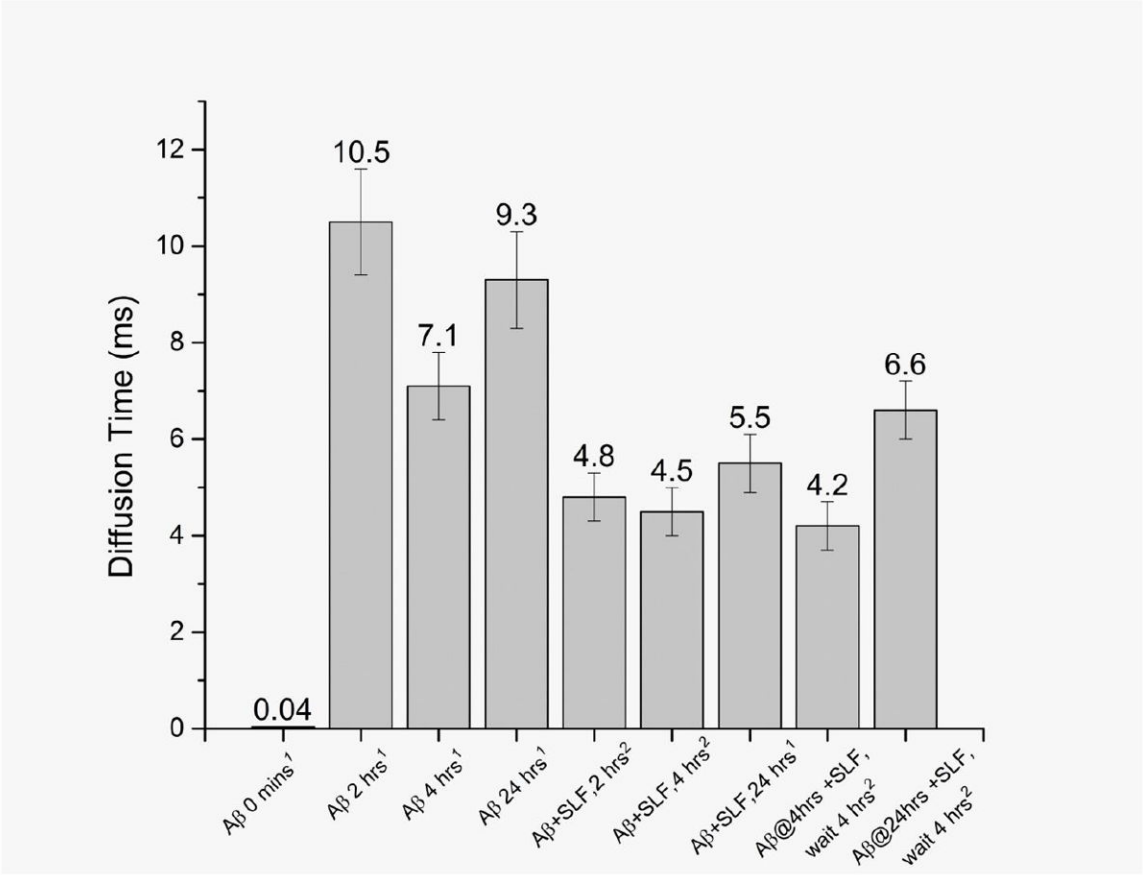

Figure 4. Diffusion times calculated from decays of FCS autocorrelation of Atto 647-labeled Aβ samples

Diffusion results are fit with [1]single-component and [2]two-component models. For the two-component fits, only the longer (τ_2) correlation time is shown. In the two-component case, τ_1 represents 15-30% of the population and is on the order of 0.1 ms (see Table S1).

Author Manuscript Author Manuscript Author Manuscript Author Manuscript

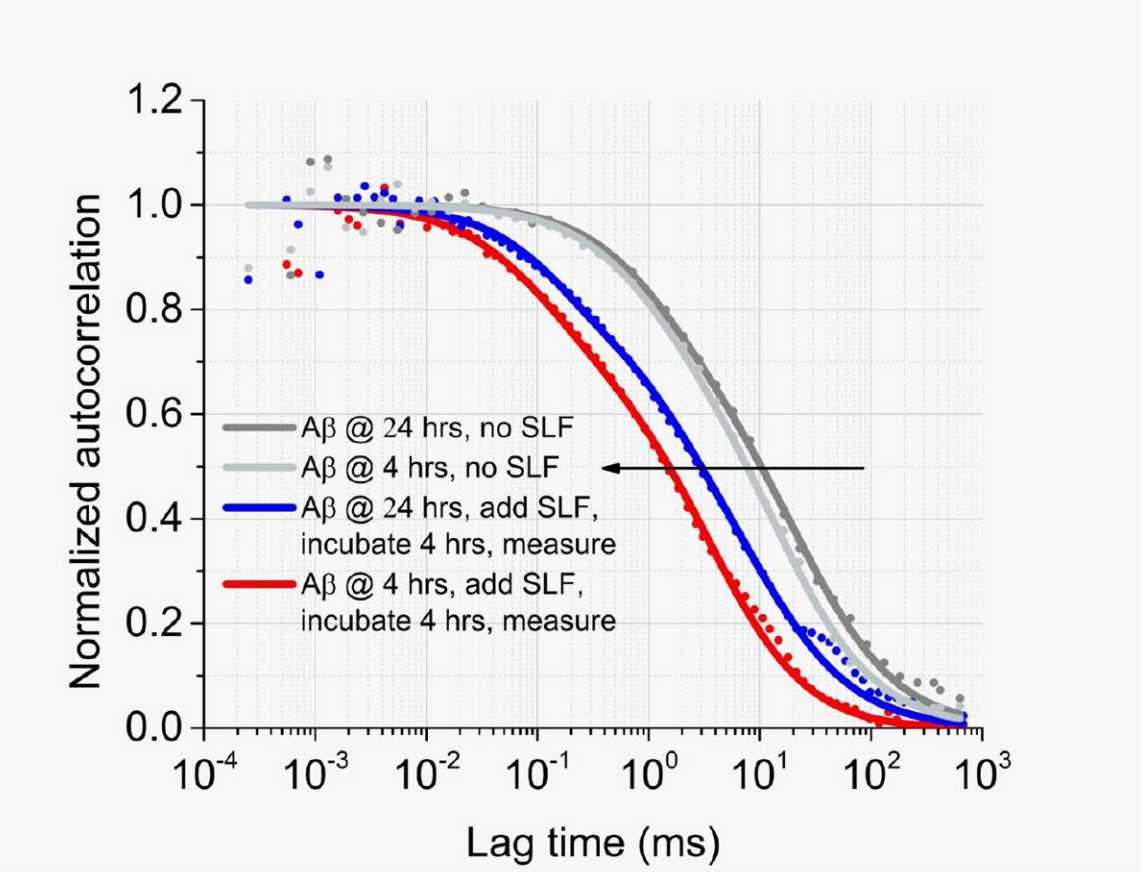

Figure 5. Effect of SLF on the FCS decay of Aβ

Shown are FCS measurements of Aβ (40 μM) following a 4-hour (light gray curve) or 24-hour (dark gray curve) incubation in PBS. Disruption of preformed AβO was probed by measuring the FCS of the 4-hour (red curve) or 24-hour (blue curve) sample following SLF treatment (40 μM), and incubating for an additional 4 hours.

Author Manuscript Author Manuscript Author Manuscript Author Manuscript

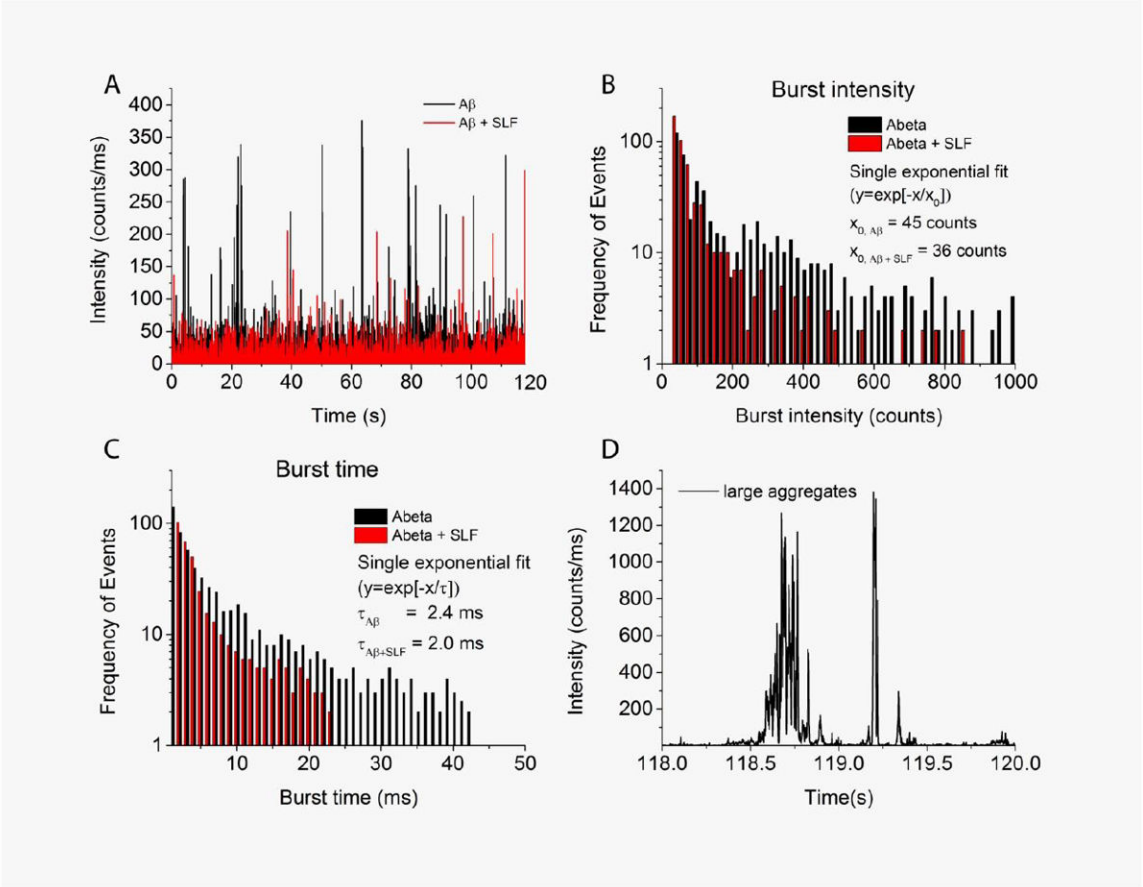

Figure 6. Photon burst analysis of Aβ and Aβ+SLF

(**A**) Fluorescence time trace of Aβ (40 μM) in the absence (black) and presence (red) of SLF (40 μM) at 4 hours. Frequency of events as a function of (**B**) burst intensity and (**C**) burst time, and fit with a single exponential decay model. In the absence of SLF, the Aβ bursts are more intense and longer in time compared with the addition of SLF. This demonstrates the presence of SLF inhibits oligomer growth. (**D**) Extremely large fluorescent bursts over 1000 counts/ms that are removed with the surface-bound species removal algorithm.

Author Manuscript Author Manuscript Author Manuscript Author Manuscript

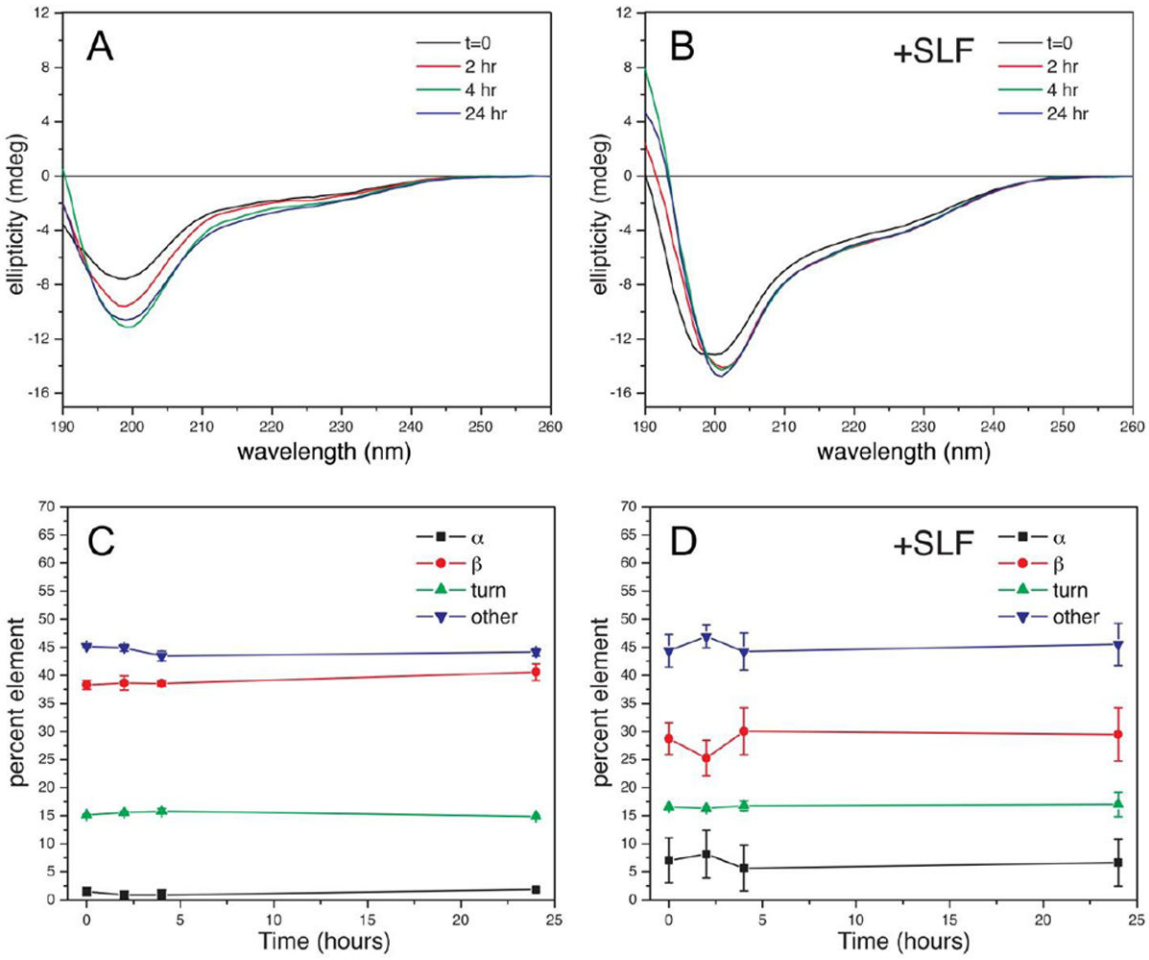

Figure 7. Time-dependent changes in the secondary structure of oligomeric Aβ

Shown are the circular dichroism (CD) spectra of Aβ (in PBS, pH 7.4) in the absence (**A**) and presence (**B**) of a stoichiometric amount of SLF. The fractions of calculated secondary structure within the peptide are shown in panels **C** (no SLF present) and **D** (40 μM SLF present). Scans were carried out on 0.1 mg/mL Aβ as described in the Methods. The BeStSel program was used for the deconvolution of secondary structure.

Author Manuscript Author Manuscript Author Manuscript Author Manuscript

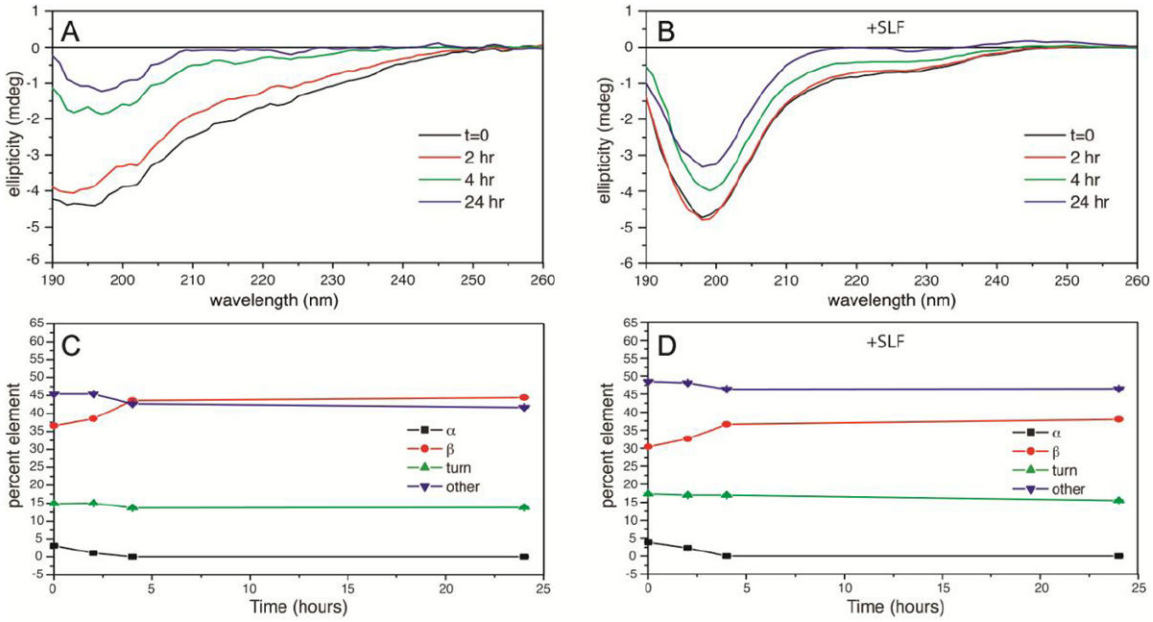

Figure 8. CD analysis of Aβ after removal of large amorphous aggregates

Shown are the circular dichroism (CD) spectra of Aβ sample supernatants (in PBS, pH 7.4) in the absence (**A**) and presence (**B**) of a stoichiometric amount of SLF following centrifugation at 15,000 × g for 5 minutes. The fractions of calculated secondary structure within the peptide are shown in panels **C** (no SLF present) and **D** (40 μM SLF present). The BeStSel program was used for the deconvolution of secondary structure.

Author Manuscript Author Manuscript Author Manuscript Author Manuscript

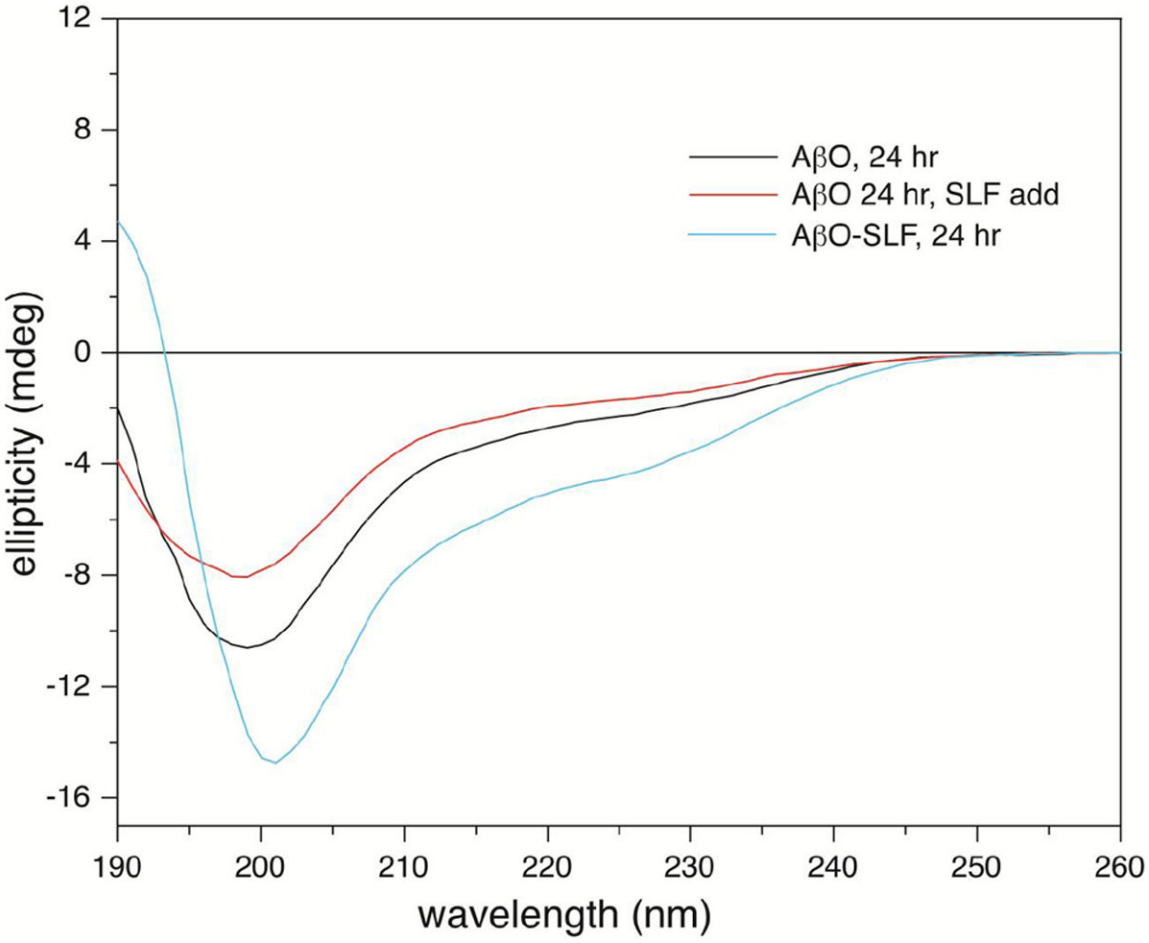

Figure 9. Effect of SLF on the secondary structure of 24-hour oligomers

CD spectrum of Aβ in PBS after 24 hours (black trace) is compared with the same sample containing addition of a stoichiometric amount of SLF at 24 hours (spectrum collected following an additional 4-hour incubation period; red curve). For comparison, the 24-hour Aβ sample containing SLF from the onset (from Figure 7) is also shown (blue trace).

Author Manuscript Author Manuscript Author Manuscript Author Manuscript

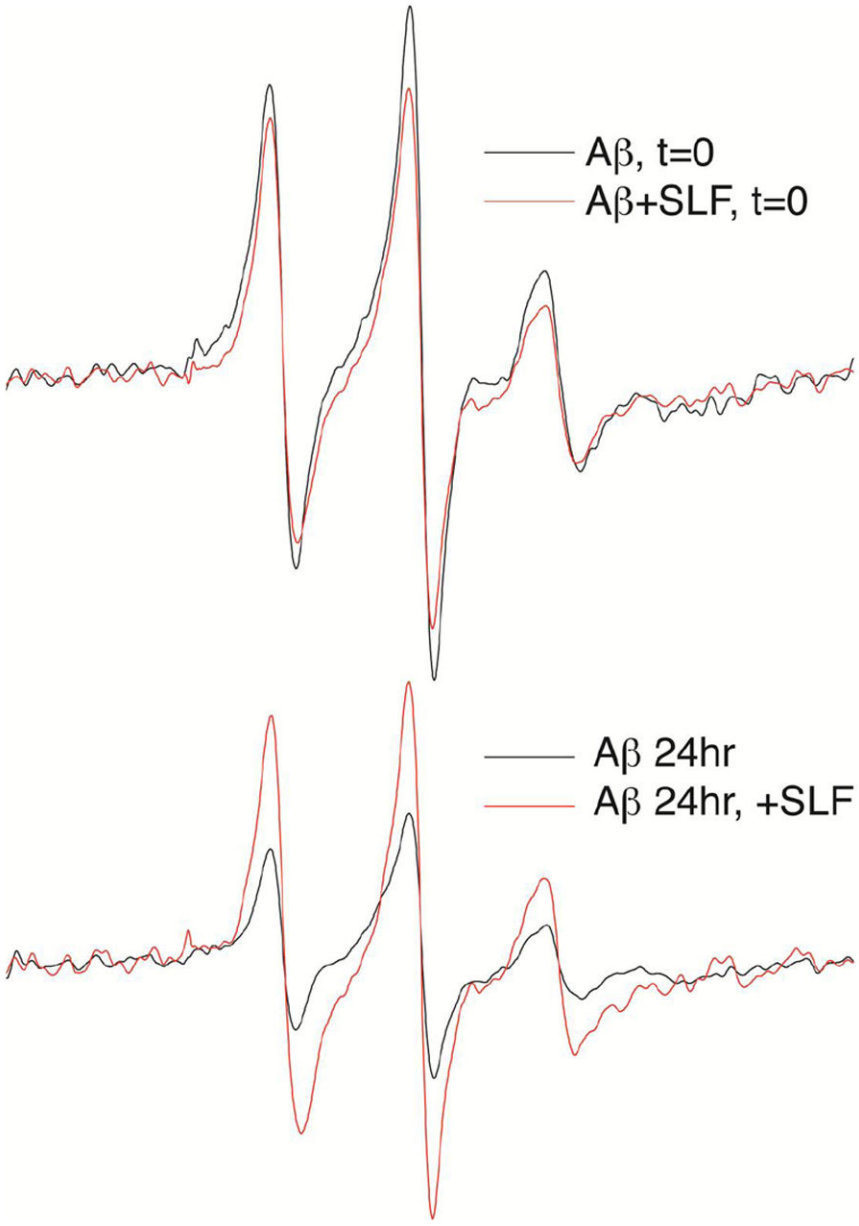

Figure 10. EPR analysis of Aβ$^{(26TOAC)}$ shows disruption of mature AβO by SLF

SLF^{dm} addition (80 μM) to a fresh preparation of Aβ in PBS buffer induces a slight broadening of the EPR line shape (**A**). Incubation of Aβ for 24 hours results in a broadened spectrum (**B**, black trace). SLF^{dm} addition (80 μM) relieves the spectral broadening (**B**, red trace), generating a signal similar to the red trace in panel (**A**). Total Aβ in each sample is 80 μM. To attenuate dipolar broadening, only 25% of the peptide is Aβ$^{(26TOAC)}$, with native Aβ$_{(1-40)}$ comprising the remaining fraction. Scans were taken over 100 G with all spectra scaled to the same number of spins.

Author Manuscript Author Manuscript Author Manuscript Author Manuscript

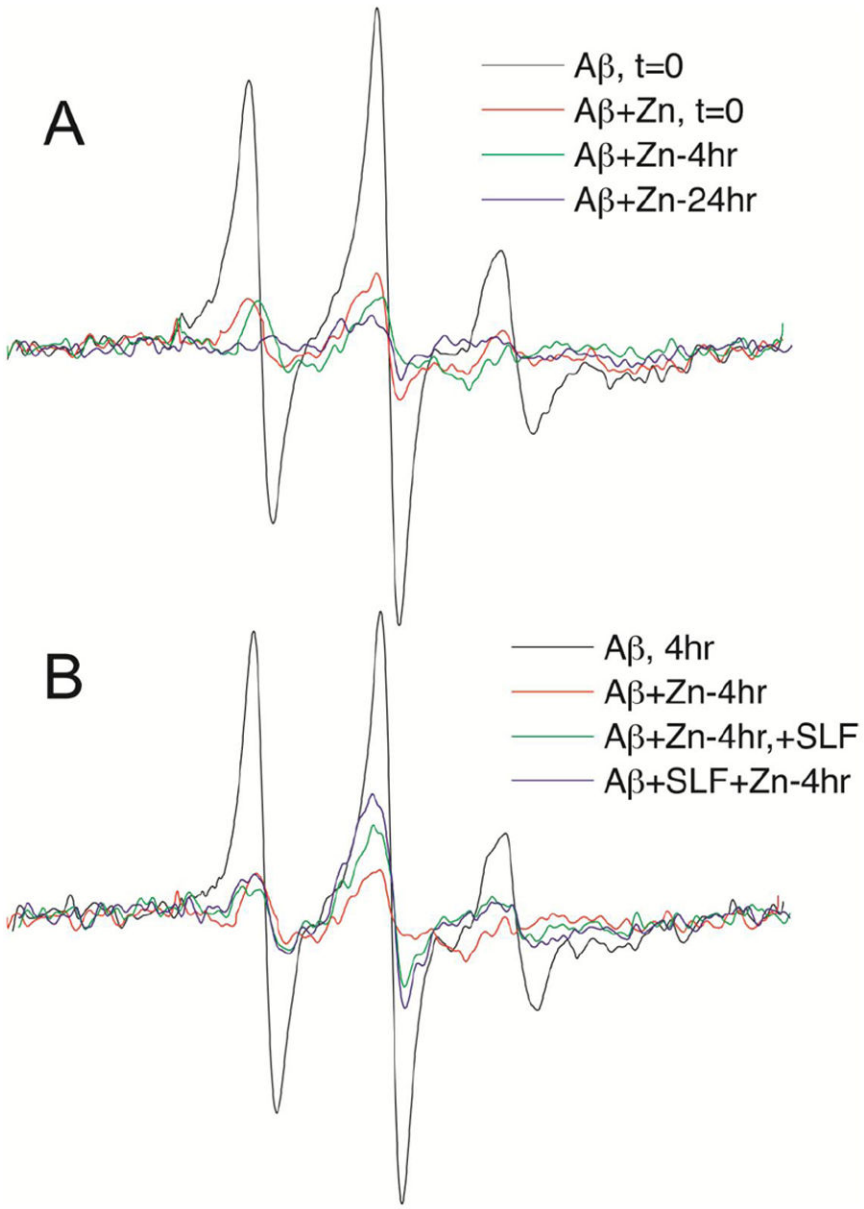

Figure 11. SLF shows a limited ability to disrupt Zinc-fortified aggregates of Aβ

The EPR spectrum of $A\beta^{(26TOAC)}$ in PBS containing 80 μM Zn(II) as a function of incubation time is shown in (**A**). In panel **B**, SLF^{dm} (80 μM) was added to the 4-hour Zn(II)-Aβ sample, incubated for 1 hour, and then scanned by EPR (green trace). The result is a slight reduction in broadening compared to the untreated Zn(II) sample at 4 hours (**B**, red trace). A similar result is found when SLF^{dm} is added prior to Zn(II) addition and the whole mixture incubated for 4 hours (**B**, blue trace). The 4-hour Aβ sample without Zn(II) is shown for comparison (**B**, black trace). Total Aβ in each sample is 80 μM. To attenuate dipolar broadening, only 25% of the peptide is $A\beta^{(26TOAC)}$, with native $A\beta_{(1-40)}$ comprising the remaining fraction. Scans were taken over 100 G with all spectra scaled to the same number of spins.